JOURNAL OF COMPUTATIONAL PHYSICS 13, 288–302 (1973)

Numerical Solutions of a Nonlinear Radiative Transfer Equation with Inadequate Data

J. SURMONT AND Y. M. CHEN

Department of Applied Mathematics and Statistics, State University of New York at Stony Brook, Stony Brook, New York 11790

Received March 30, 1973

Iterative algorithms for solving numerically a nonlinear radiative transfer equation with inadequate data are presented and tested by numerical simulations. It is found that these iterative algorithms do give excellent results.

1. INTRODUCTION

Remote sensing problems in atmospheric, oceanic, and geophysical sciences can be formulated often as "improperly posed" problems in mathematical analysis. To solve these problems is equivalent to constructing approximate solutions of operator equations, whose solutions often are nonunique and do not depend continuously on the given data, from inadequate (or insufficient) data with or without errors. Since early nineteen sixties, various inversion techniques have been developed for these problems [see, for example, Fleming and Smith [1], Conrath and Revah [2] (excellent reviews), Backus and Gilbert [3–5], Franklin [6], Tihonov [7, 8], Lavrentiev [9, 10], etc.]. In particular, the method of Backus and Gilbert (B & G) not only provides an inversion technique but also can be used as a diagnostic tool for testing the intrinsic resolution of a given set of data for a given problem. Although B & G's inversion technique is applicable to nonlinear problems, it does not appear to be fully developed, and in this regard, two iterative algorithms for constructing approximate solutions of nonlinear problems from inadequate data have been presented and their theoretical aspect has been discussed by Chen and Surmont [11] recently.

It is the purpose of the present paper to demonstrate the applicability of the two iterative algorithms of Chen and Surmont [11] to a nonlinear radiative transfer equation with inadequate data, which is often encountered in the remote sensing of atmospheric temperature profiles. In particular, radiance measurements in two CO_2 absorption bands (15 μm and 4.3 μm), observed by the High Resolution Infrared Radiation Sounder (HIRS) of the National Oceanic and Atmospheric

Administration, within a nonscattering atmosphere in local thermodynamic equilibrium are employed. Upon using the technique of B & G (equivalent to the first iteration of the iterative algorithms of Chen and Surmont [11]), Conrath [12] has calculated the intrinsic vertical resolution of temperature profiles obtained from remote radiation measurements in the 15 μm CO_2 absorption band. Similarly, Chen, Woolf, and Smith [13] have obtained the intrinsic resolutions of temperature profiles obtained from remote radiation measurements in the 4.5 μm, 15 μm, and 4.3 μm + 15 μm CO_2 bands separately, and it is found that the combination of 4.3 μm and 15 μm bands is superior to the other two individual cases for all levels of the pressure, especially in the upper troposphere and the stratosphere.

A brief review of the formulation of B & G in terms of the nonlinear radiative transfer equation is given in the next section. Next, the iterative algorithms of [11] are presented in Section 3. Then discussion and comparison are made in the last section. Finally, the Appendix serves partially as a bridge between the theoretical aspect of [11] and the practical aspect of the particular nonlinear radiative transfer equation in this paper. It should be noted that the following computational formulations can be applied directly to noisy data only if they are properly modified [5, 11].

2. The Method of Backus and Gilbert

For a nonscattering atmosphere in local thermodynamic equilibrium, the radiation emitted at frequency ν is given by the integral form of the radiative transfer equation,

$$I(\nu) = B[T(p_0), \nu]\, \tau(p_0, \nu) - \int_0^{p_0} B[T(p), \nu] \frac{d\tau(p, \nu)}{dx(p)}\, dx(p), \tag{1}$$

where

$$\begin{aligned} B[T(p), \nu] &= c_1\nu^3/\{\exp[c_2\nu/T(p)] - 1\}, \\ c_1 &= 1.19061 \times 10^{-5}\ \text{erg-cm}^2\text{-sec}^{-1}, \\ c_2 &= 1.43868\ \text{cm-deg(K)} \end{aligned} \tag{2}$$

is the Planck function for the temperature $T(p)$ at the pressure p (in mb); the independent variable x can be any monotonic function of p ($x = \ln p$ being used here); p_0 is the surface pressure; and $\tau(p, \nu)$ is the transmittance of the atmosphere above pressure p at ν.

In the remote sensing of the atmospheric temperature profiles, measurements of radiances in a finite number of spectral intervals within atmospheric absorption bands are performed. The inversion problem then is to estimate the temperature profile $T(p)$, given the atmospheric transmittances $\tau(p, \nu)$ and measurements of the radiances $\{I(\nu_i)\}$, $i = 1, 2,..., m$. If the contribution from the nonlinearity of (1) is small, then only the first iteration of the iterative algorithms of Chen and Surmont [11] or the procedure of B & G [3–5] will be sufficient for our purpose. Let

$$T(p) \simeq T_0(p) + \hat{T}_1(p), \tag{3}$$

where $T_0(p)$ is the initial or reference profile and is taken to be the U.S. standard atmosphere. Then from [11], $\hat{T}_1(p)$ should be the solution of the linearized equation

$$\int_{-\infty}^{x_0} K[x, \nu_i]\, \hat{T}_1(x)\, dx = \delta I(\nu_i), \qquad i = 1, 2,..., m, \tag{4}$$

where

$$K[x, \nu_i] = \frac{dB[T(x), \nu_i]}{dT}\bigg|_{T_0} \frac{d\tau(x, \nu_i)}{dx}, \tag{5}$$

$$\delta I(\nu_i) = B[T_0(x_0), \nu_i]\, \tau(x_0, \nu_i) - \int_{-\infty}^{x_0} B[T_0(x), \nu_i] \frac{d\tau(x, \nu_i)}{dx} - I(\nu_i), \tag{6}$$

and dB/dT is the functional derivative of $B[T]$. It can be shown that the integral operator of (1) has Fréchet derivatives when $T(x)$ belongs to C, the space of continuous functions (Appendix).

The weighted average of $\hat{T}_1$ at x which gives heavy emphasis to points close to x and very little to distant points is defined by

$$\langle \hat{T}_1 \rangle_x = \int_{-\infty}^{x_0} A(x, x')\, \hat{T}_1(x')\, dx'), \tag{7}$$

where the averaging kernel A is normalized according to

$$\int_{-\infty}^{x_0} A(x, x')\, dx' = 1. \tag{8}$$

It is obvious that $\langle \hat{T}_1 \rangle_x$ is the most localized weighted average if and only if the averaging kernel A resembles the Dirac delta function $\delta(x' - x)$ most closely. The spread of A from x is defined by

$$Q(x, A) \equiv \alpha_J \int_{-\infty}^{x_0} J(x, x')\, A^2(x, x')\, dx', \tag{9}$$

where $J(x, x')$ is a chosen infinitely differentiable function of x' such that $J(x, x) = 0$

and increases monotonically as x' increases or decreases away from x with dimension of $(x')^2$, and

$$\alpha_J = \frac{l}{\int_{-\infty}^{x_0} J(x, x')\, A_l^2(x, x')\, dx'} \tag{10}$$

with

$$A_l(x, x') = \begin{cases} 1/l, & x - l/2 < x' < x + l/2, \\ 0, & | x' - x | \geqslant l/2. \end{cases} \tag{11}$$

Note that

$$Q(x, A_l) = l \qquad \text{(the spread of } A_l\text{)}. \tag{12}$$

Actually, if A has a sharp peak, the choice of J is rather free. However, if A has a blurred peak, the selection of J is much more critical. Throughout,

$$J(x, x') = (x - x')^2 \tag{13}$$

is used and then $\alpha_J = 12$.

Equation (4) shows that $\{\delta I(\nu_i)\}$, $i = 1, 2,..., m$, are m bounded linear functionals of $\hat{T}_1(x)$. Since $\langle \hat{T}_1 \rangle_x$ and $\{\delta I(\nu_i)\}$, $i = 1, 2,..., m$, all depend linearly on the function $\hat{T}_1$, it follows that $\langle \hat{T}_1 \rangle_x$ must depend linearly on $\{\delta I(\nu_i)\}$, $i = 1, 2,..., m$. Therefore, there should exist constants $\{a_i(x)\}$, $i = 1, 2,..., m$, depending on the fixed point x such that

$$\langle \hat{T}_1 \rangle_x = \sum_{i=1}^{m} a_i(x)\, \delta I(\nu_i). \tag{14}$$

Hence, from (4) and (7),

$$A(x, x') = \sum_{i=1}^{m} a_i(x)\, K[x', \nu_i]. \tag{15}$$

It follows from (9) and (15) that $Q(x, A)$ is a positive-definite quadratic function of $\{a_i(x)\}$, $i = 1, 2,..., m$. Since the determination of the most localized weighted average $\langle \hat{T}_1 \rangle_x$ is equivalent to minimizing the spread of A from x subject to the constraint (8), by using the method of Lagrange multipliers, the proper set of $\{a_i(x)\}$, $i = 1, 2,..., m$, satisfies the following set of $m + 1$ linear algebraic equations:

$$\begin{aligned} &\sum_{j=1}^{m} \left\{ 24 \int_{-\infty}^{x_0} (x - x')^2 K[x', \nu_i]\, K[x', \nu_j]\, dx' \right\} a_j(x) + \lambda \int_{-\infty}^{x_0} K[x', \nu_i]\, dx' = 0, \\ &\qquad\qquad\qquad\qquad\qquad\qquad\qquad\qquad i = 1, 2,..., m, \\ &\sum_{j=1}^{m} \left\{ \int_{-\infty}^{x_0} K[x', \nu_j]\, dx' \right\} a_j(x) = 1, \end{aligned} \tag{16}$$

where λ is a Lagrange multiplier.

The vertical resolution of the temperature profile at the level x obtainable from a given set of radiance measurement is determined by the closeness of $A(x, x')$ to $\delta(x' - x)$. Visually, the plot of $A(x, x')$ vs x' gives a qualitative estimate of the vertical resolution at x. To characterize the behavior of $A(x, x')$ more precisely, the "resolving length" of $A(x, x')$ is introduced and defined as the spread about its center,

$$w(x) = 12 \int_{-\infty}^{x_0} [c(x) - x']^2 A^2(x, x')\, dx, \tag{17}$$

where

$$c(x) = \int_{-\infty}^{x_0} x' A^2(x, x')\, dx' \Big/ \int_{-\infty}^{x_0} A^2(x, x')\, dx' \tag{18}$$

is the "center" of $A(x, x')$.

The center frequencies of the seven channels ($i = 1,\ldots, 7$) in the 15 μm CO_2 band and the five channels ($i = 8,\ldots, 12$) in the 4.3 μm CO_2 band in our study are 668.5, 680.0, 690.0, 703.0, 716.0, 733.0, 749.0 (cm^{-1}) and 2190.0, 2210.0, 2240.0, 2270.0, 2360.0 (cm^{-1}), respectively. The numerical data of $\tau(x_k, \nu_i)$ and $d\tau(x, \nu_i)/dx\,|_{x=x_k}$, $i = 1, 2,\ldots, 12$, $k = 1, 2,\ldots, 200$, are furnished by the National Environmental Satellite Service, NOAA, and the $d\tau(x, \nu_i)/dx(p)$ vs p curves are given in Figs. 1 and 2 of [13]. The integration is performed numerically by using the Simpson's rule. The integration limits are -2.3026 and 6.9078 ($\simeq x_0$) instead of $-\infty$ and 6.9078. This is because the $d\tau(x, \nu_i)/dx$, $i = 1, 2,\ldots, 12$, are negligible for $x < -2.3$.

3. Iterative Algorithms and Numerical Solutions

Two iterative algorithms [11] for constructing approximate solutions of the nonlinear radiative transfer equation (1) from inadequate data will be presented here. These algorithms are basically hybrids of Newton's iterative methods in Banach spaces [14] and the inversion technique of B & G described in the previous section.

Method I (*Modified Nexton's Method*)

The $(n + 1)$th approximate solution of (1) is defined by

$$\langle T_{n+1}\rangle_x \equiv T_0(x) + \sum_{j=0}^{n} \langle T_{j+1} - T_j\rangle_x, \qquad n = 0, 1, 2,\ldots, \tag{19}$$

where $\langle T_{n+1} - T_n \rangle_x$, assumed to be unique, is the best approximate solution (in the sense of B & G) of the linearized equation,

$$\int_{-\infty}^{x_0} \frac{dB[T(x), \nu]}{dT}\bigg|_{T_0(x)} \frac{d\tau(x, \nu)}{dx} [T_{n+1}(x) - T_n(x)]\, dx$$

$$= B[\langle T_n \rangle_{x_0}, \nu]\, \tau(x_0, \nu) - \int_{-\infty}^{x_0} B[\langle T_n \rangle_x, \nu] \frac{d\tau(x, \nu)}{dx}\, dx - I(\nu), \tag{20}$$

where

$$\frac{dB[T(x), \nu]}{dT} = \frac{c_1 c_2 \nu^4 \exp[c_2 \nu / T(x)]}{[T(x)]^2 \{\exp[c_2 \nu / T(x)] - 1\}^2}, \tag{21}$$

from the given inadequate data $I(\nu_i)$ $i = 1, 2, \ldots, 12$.

Method II (*Newton's Method*)

The $(n + 1)$th approximate solution of (1) is defined by

$$\langle \mathbf{T}_{n+1} \rangle_x \equiv T_0(x) + \sum_{j=0}^{n} \langle \mathbf{T}_{j+1} - \mathbf{T}_j \rangle_x, \qquad n = 0, 1, 2, \ldots, \tag{22}$$

where $\langle \mathbf{T}_{n+1} - \mathbf{T}_n \rangle_x$, assumed to be unique, is the best approximate solution of the linearized equation

$$\int_{-\infty}^{x_0} \frac{dB[T(x), \nu]}{dT}\bigg|_{\langle \mathbf{T}_n \rangle_x} \frac{d\tau(x, \nu)}{dx} [\mathbf{T}_{n+1}(x) - \mathbf{T}_n(x)]\, dx$$

$$= B[\langle \mathbf{T}_n \rangle_{x_0}, \nu]\, \tau(x_0, \nu) - \int_{-\infty}^{x_0} B[\langle \mathbf{T}_n \rangle_x, \nu] \frac{d\tau(x, \nu)}{dx}\, dx - I(\nu) \tag{23}$$

from the given inadequate data $\{I(\nu_i)\}$, $i = 1, 2, \ldots, 12$.

Due to great difficulties in obtaining the estimates of the various operators in the theorems [11], it is futile to apply these theorems directly in practice. Instead, one has to evaluate the performance of the above two iterative algorithms numerically. Since the HIRS is not in operation yet to provide the real measurements of the radiances $I(\nu_i)$, $i = 1, \ldots, 12$, a numerical simulation must be carried out. The procedure is that, the solution of the nonlinear radiative transfer equation (1), $T(x)$, is first assumed and then Eq. (1) is numerically integrated to give $I(\nu_i)$; from these radiances, an approximate solution of (1), $\langle T^* \rangle_x$, is obtained by using either one of the above two iterative algorithms. Other than the round-off and numerical integration errors, the quantity $\| T(x) - \langle T^* \rangle_x \|$ can be used as a criterion for evaluating the performance of the iterative algorithm. Although only functions in C are considered, L^2 norm is used here because of its integrated effect.

With double precision in the computation, four examples, (a) smooth $T(x)$ with small $\| T(x) - T_0(x)\|$, (b) zigzag $T(x)$ with small $\| T(x) - T_0(x)\|$, (c) smooth $T(x)$ with large $\| T(x) - T_0(x)\|$, and (d) zigzag $T(x)$ with large $\| T(x) - T_0(x)\|$, are tried and their numerical results are plotted in Figs. 1, 2, 3 and 4, respectively.

4. Discussion

For the case (a), Fig. 1 shows that the accuracy of ten iterations of Method I ($i = 1,..., 12$) is equivalent to three iterations of Method II ($i = 1,..., 12$). This means that Method II converges faster than Method I. However, the computation

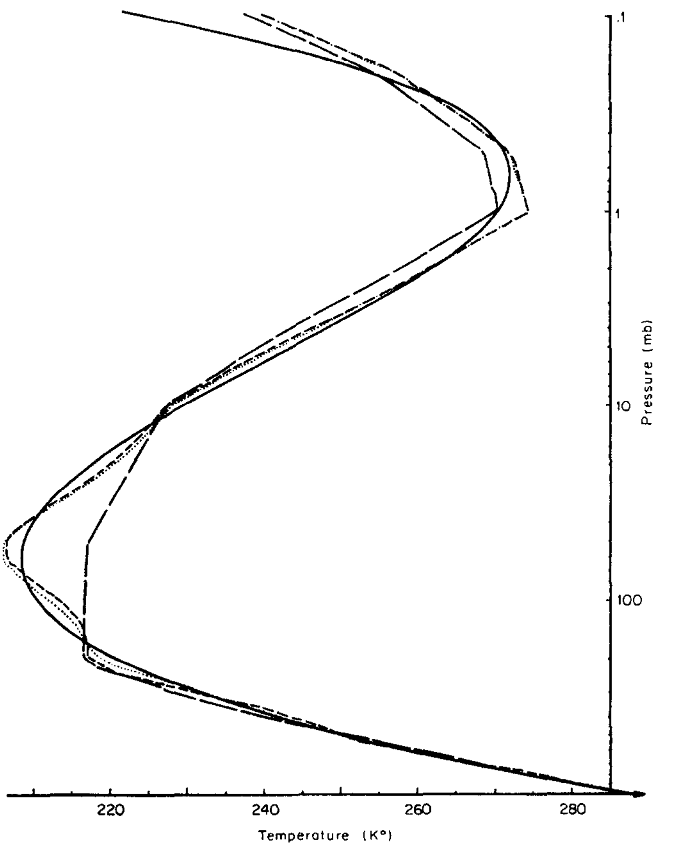

FIG. 1. Comparison of Methods I and II for smooth $T(p)$ with small $\| T(p) - T_0(p)\|$ and $i = 1, 2,..., 12$. — T; --- T_0 ; - - - $\langle T_3 \rangle$, $i = 1,..., 12$; ···· $\langle T_{10} \rangle$, $i = 1,... 12$.

is longer for obtaining $\langle \mathbf{T}_3 \rangle_x$ than $\langle T_{10} \rangle_x$. The approximate solutions are extremely good for $1000 \text{ mb} \geqslant p > 200 \text{ mb}$, uniformly and reasonably good for $200 \text{ mb} > p > 0.2 \text{ mb}$. Upon examining the numerically computed norms $\| T - \langle T_n \rangle \|$, $\| T - \langle \mathbf{T}_n \rangle \|$, $\| \langle T_{n+1} \rangle - \langle T_n \rangle \|$ and $\| \langle \mathbf{T}_{n+1} - \langle \mathbf{T}_n \rangle \|$, and Figs. 1–4, it is found that both iterative algorithms converge to the same limit $\langle T^* \rangle_x$.

For the case (b), Fig. 2 shows again that the accuracy of $\langle T_{10} \rangle_x$ is approximately equivalent to that of $\langle \mathbf{T}_3 \rangle_x$, and it takes longer to compute $\langle \mathbf{T}_3 \rangle_x$ than $\langle T_{10} \rangle_x$. Again both iterative algorithms converge to the same limit $\langle T^* \rangle_x$. These approximate solutions are remarkably good for $1000 \text{ mb} \geqslant p > 200 \text{ mb}$ (even catching the temperature inversion) and reasonably good for $200 \text{ mb} > p > 0.3 \text{ mb}$.

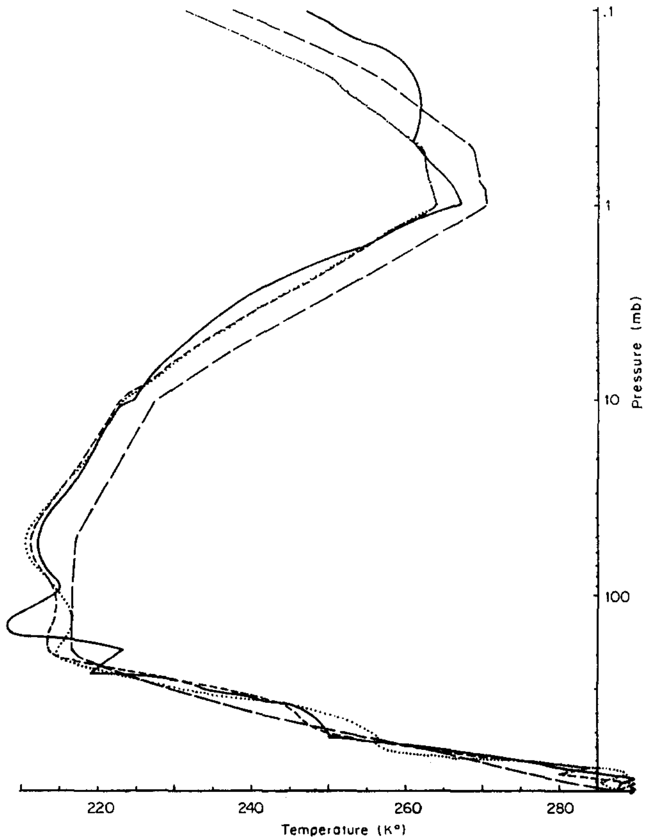

FIG. 2. Comparison of Methods I and II for zigzag $T(p)$ with small $\| T(p) - T_0(p) \|$ and $i = 1, 2, \ldots, 12$. — T; — — — T_0; - - - $\langle T_{10} \rangle$, $i = 1, \ldots, 12$; ··· $\langle \mathbf{T}_3 \rangle$, $i = 1, \ldots 12$.

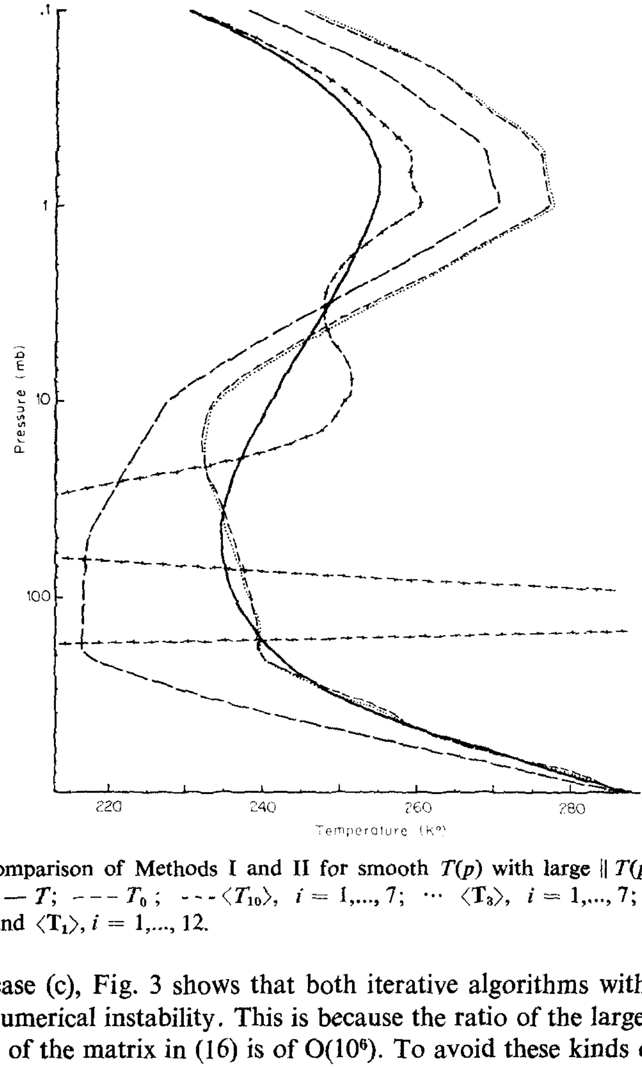

FIG. 3. Comparison of Methods I and II for smooth $T(p)$ with large $\| T(p) - T_0(p)\|$ and $i = 1, 2,..., 7$. — T; - - - T_0 ; - - - $\langle T_{10}\rangle$, $i = 1,..., 7$; ··· $\langle T_3\rangle$, $i = 1,..., 7$; + + + $\langle T_1\rangle$, $i = 1,..., 12$ and $\langle T_1\rangle$, $i = 1,..., 12$.

For the case (c), Fig. 3 shows that both iterative algorithms with $i = 1,..., 12$ encounter numerical instability. This is because the ratio of the largest element to the smallest of the matrix in (16) is of $O(10^6)$. To avoid these kinds of difficulties, both iterative algorithms with $i = 1,..., 7$ are used. Again it is found that $\langle T_3\rangle_x$ $(i = 1,..., 7) \simeq \langle T_{10}\rangle_x$ $(i = 1,..., 7)$ and both iterative algorithms converge to the same limit $\langle T^*\rangle_x$. These approximate solutions with $i = 1,..., 7$ are remarkably good for 1000 mb $\geqslant p >$ 200 mb, reasonably good for 200 mb $> p >$ 30 mb and poor for $p <$ 30 mb. It is interesting to notice that $\langle T_1\rangle_x$ $(i = 1,..., 12)$ is a much better approximation in the range, 0.1–5 mb, than either $\langle T_3\rangle_x$ $(i = 1,..., 7)$ or $\langle T_{10}\rangle_x$ $(i = 1,..., 7)$, before it encounters the numerical instability in the range, 5–1000 mb. This is understandable, because 12 channels has better performance index (weighted linear combination of resolving length and correct centering) in the upper stratosphere than that of seven channels [13]. This shows that for the case of 12 channels (4.3 μm + 15 μm CO_2 bands), if the initial guess $T_0(x)$ deviates very much from the true solution $T(x)$, the iterative algorithms are more likely to encounter the difficulty of numerical instability; however, if only seven channels (15 μm CO_2 band) are used, the aforementioned numerical instability will not be encountered. Similarly, this is true for the case (d) (Fig. 4).

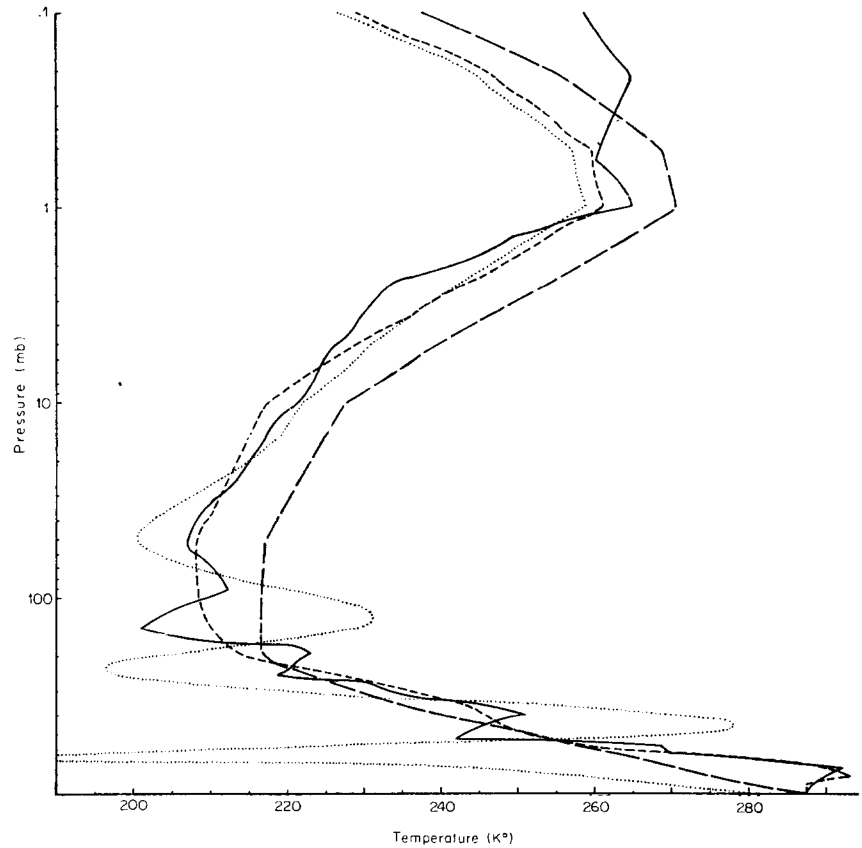

FIG. 4. $\langle T \rangle_p$ obtained by Method I for zigzag $T(p)$ with large $\| T(p) - T_0(p) \|$ and $i = 1, 2, \ldots, 7$. — T; – – – T_0 ; - - - $\langle T_{10} \rangle$, $i = 1, \ldots, 7$; ··· $\langle T_1 \rangle$, $i = 1, \ldots, 12$, and $\langle T_1 \rangle$, $i = 1, \ldots, 12$.

Samples of numerically computed L^2 norms are given in Table I.

In view of the previous discussion, Method I is better than Method II in actual computation. The best practical approach is to use Method I with seven channels

TABLE I

Samples of Numerically Computed L^2 Norms

	Case a $i = 1, 2, \ldots, 12$		Case b $i = 1, 2, \ldots, 12$		Case c $i = 1, 2, \ldots, 7$			
n	$\lVert T - \langle T_n \rangle \rVert$	$\lVert \langle T_n \rangle - \langle T_{n-1} \rangle \rVert$	$\lVert T - \langle T_n \rangle \rVert$	$\lVert \langle T_n \rangle - \langle T_{n-1} \rangle \rVert$	$\lVert T - \langle T_n \rangle \rVert$	$\lVert \langle T_n \rangle - \langle T_{n-1} \rangle \rVert$	$\lVert T - \langle \mathbf{T}_n \rangle \rVert$	$\lVert \langle \mathbf{T}_n \rangle - \langle \mathbf{T}_{n-1} \rangle \rVert$
0	415.0		674.0		3560.0		3560.0	
1	219.0	177.0	596.0	554.0	3194.0	3542.0	3194.0	3542.0
2	213.0	16.0	445.0	169.0	2479.0	96.0	2446.0	77.0
3	200.0	3.0	462.0	8.0	2423.0	2.0	2342.0	0.3
4	190.0	1.30	484.0	10.0	2381.0	0.5		
5	183.0	0.7	506.0	5.0	2365.0	0.11		
6	179.0	0.4	499.0	0.5	2355.0	0.06		
7	176.0	0.3	492.0	0.8	2349.0	0.03		
8	175.0	0.2	489.0	0.4	2344.0	0.02		
9	173.0	0.15	488.0	0.3	2341.0	0.01		
10	173.0	0.11	487.0	0.2	2339.0	0.006		

for the first few iterations to avoid possible numerical instability and then to switch to Method I with 12 channels to catch the fine details of the approximate solutions.

APPENDIX

The fact that if the solutions of (1) belong to $C[a, b]$, then that nonlinear integral operator has Fréchet derivative will be shown in the following: Let

$$N[u, \nu] \equiv B[u(b), \nu]\, \tau(b, \nu) - \int_a^b B[u(x), \nu] \frac{\partial \tau}{\partial x}(x, \nu)\, dx,$$

$$D : a \leqslant x \leqslant b, \qquad c \leqslant \nu \leqslant d, \qquad 0 < u < \infty,$$

$T(b, \nu)$ be continuous on $[c, d]$, and

$\partial\tau(x, \nu)/\partial x$ be continuous on $[a, b] \times [c, d]$.

Then

$$K(x, \nu, u) \equiv B[u, \nu]\, \partial\tau(x, \nu)/\partial x,$$

$$K_u'(x, \nu, u) = \frac{c_1 c_2 \nu^4 \exp[c_2\nu/u(x)]}{u^2(x)\{\exp[c_2\nu/u(x)] - 1\}^2} \frac{\partial\tau(x, \nu)}{\partial x},$$

$$K_b(\nu, u) \equiv B[u(b), \nu]\, \tau(b, \nu), \qquad \text{and}$$

$$(K_b)_u'(\nu, u) = \frac{c_1 c_2 \nu^4 \exp[c_2\nu/u(b)]}{u^2(b)\{\exp[c_2\nu/u(b)] - 1\}^2} \tau(b, \nu)$$

are continuous on D. Let

$$u(x) \in \Omega\{u \in C[a, b];\ u > 0 \text{ for every } x \in [a, b]\} \subset B_1 \equiv C[a, b]$$

and

$$I(\nu) \in B_2 \equiv C[c, d].$$

Then the nonlinear integral operator of (1),

$$P[u, \nu] \equiv N[u, \nu] - I(\nu) \text{ maps } \Omega \text{ into } B_2 .$$

THEOREM. *For every* $\mathbf{u}(x) \in \Omega$ *and every* $v(x) \in B_1$, $P_u'[\mathbf{u}, \nu]$ $(B_1 \to B_2)$ *is the Fréchet derivative of* $P[u, \nu]$ *at* $\mathbf{u}(x)$, *where*

$$P_u'[\mathbf{u}, \nu] \cdot v(x) = (K_b)_u'(\nu, \mathbf{u}) \cdot v(b) - \int_a^b K_u'(x, \nu, \mathbf{u}) \cdot v(x)\, dx.$$

Proof. It follows from the continuity of $(K_b)_u'(u, \nu)$ and $K_u'(x, \nu, u)$ that $P_u'[\mathbf{u}, \nu]$ maps B_1 into B_2.

From the expression of $P_u'[\mathbf{u}, \nu]$ above, it is obviously a linear operator. Next, from the definition of $P_u'[\mathbf{u}, \nu]$,

$$\| P_u' \cdot v \| = \max_{\nu} | P_u' \cdot v | \leqslant (L_1 + L_2) \max_x | v(x)| \leqslant (L_1 + L_2)\| v \|,$$

where

$$L_1 = \frac{K_1 c_1 c_2 d^4 \exp[c_2 d/\mathbf{u}(b)]}{\mathbf{u}^2(b)\{\exp[c_2 c/\mathbf{u}(b)] - 1\}^2},$$

$$L_2 = \frac{K_2 c_1 c_2 d^4 \exp[c_2 d/m](b - a)}{m^2\{\exp[c_2 c/M] - 1\}^2},$$

$$K_1 = \max_{\nu} | \tau(b, \nu)|,$$

$$K_2 = \max_{x,\nu} | \partial\tau(x, \nu)/\partial x |,$$

$$m = \min_x \mathbf{u}(x) \qquad \text{and} \qquad \max_x \mathbf{u}(x) = M.$$

Hence, $P_u'[\mathbf{u}, \nu]$ is bounded.

Finally, to show that

$$\| E \| \equiv \left\| P_u'[\mathbf{u}] \cdot v - \frac{P[\mathbf{u} + tv] - P[\mathbf{u}]}{t} \right\| \to 0 \qquad \text{for} \quad t \to 0$$

uniformly with respect to $v(x)$ where $\| v \| = 1$, from the definitions, one obtains

$$| E | \leqslant \left| (K_b)_u'(\nu, \mathbf{u}) \cdot v(b) - \frac{K_b(\nu, \mathbf{u} + tv) - K_b(\nu, \mathbf{u})}{t} \right|$$
$$+ \left| \int_a^b \left\{ K_u'[x, \nu, \mathbf{u}] \cdot v(x) - \frac{K[x, \nu, \mathbf{u} + tv] - K[x, \nu, \mathbf{u}]}{t} \right\} dx \right|$$
$$\equiv | E_1 | + | E_2 |.$$

Then

$$| E_1 | \leqslant | v(b)| \left| (K_b)_u'(\nu, \mathbf{u}) - \frac{K_b(\nu, \mathbf{u} + \tau) - K_b(\nu, \mathbf{u})}{\tau} \right|, \qquad \tau = tv(b)$$
$$= | v(b)| |(K_b)_u' - (K_b)'_{u+\theta\tau} |, \quad 0 \leqslant \theta \leqslant 1, \quad \text{by the mean-value theorem},$$
$$\leqslant \max_x | v(x)| \, \epsilon_1 = \epsilon_1 \| v \|, \qquad \text{for} \quad | \tau | = t \, | v(b)| < \delta_1,$$

due to the continuity of $(K_b)_u'$.

Similarly, $| E_2 | \leqslant \epsilon_2(b - a) \| v(x)\|$, for $| \tau(x)| = | t | \, | v(x)| < \delta_2$. Then $| E | \leqslant [\epsilon_1 + (b - a)\epsilon_2] \| v(x)\| = \epsilon \| v \|$, for every $\nu \in [c, d]$. That is

$$\left\| P_u'[\mathbf{u}] \cdot v - \frac{P[\mathbf{u} + tv] - P[\mathbf{u}]}{t} \right\| \leqslant \epsilon \| v \| \qquad \text{for} \quad | t | < \delta_1 ; \delta_2 .$$

Since $\| v(x)\| = 1$, the above statement is equivalent to the statement which we want to show. Hence, by the definition of the Fréchet derivative [14], the theorem is proved.

Acknowledgment

This research has been supported in part by the Atmospheric Sciences Section, National Science Foundation, Grant No. A035613.

References

1. H. E. Fleming and W. L. Smith, Inversion techniques for remote sensing of atmospheric Temperature profiles, "Proceedings of the Fifth Symposium on Temperature, Its Measurement and Control in Science and Industry," Washington, DC, June, 1971.
2. B. J. Conrath and I. Revah, "A Review of Nonstatistical Techniques for the Estimation of Vertical Atmospheric Structure From Remote Infrared Measurements," "Proceedings of a Workshop on the Mathematics of Profiles Inversion," (L. Colin, Ed.), Ames Research Center, NASA, July, 1971.
3. G. Backus and F. Gilbert, Numerical applications of a formalism for geophysical inverse problems, *Geophys. J. Roy. Astron. Soc.* **13** (1967), 247–276.
4. G. Backus and F. Gilbert, The resolving power of gross earth data, *Geophys. J. Roy. Astron. Soc.* **16** (1968), 169–205.
5. G. Backus and F. Gilbert, "Uniqueness in the Inversion of Inaccurate *G*oss Earth Data," *Philos. Trans. Royal Soc. Ser. A* **266** (1970), 123–192.
6. J. N. Franklin, Well-posed stochastic extensions of ill-posed linear problems, *J. Math. Anal. Appl.* **31** (1970), 682–716.
7. A. N. Tihonov, Solution of incorrectly formulated problems and the regularization method, *Soviet Math. Dokl.* **4** (1963), 1035–1038.
8. A. N. Tihonov, Nonlinear equations of the first kind, *Soviet Math. Dokl.* **6** (1965), 559–562.
9. M. M. Lavrentiev, "Some Improperly Posed Problems of Mathematical Physics," Springer Tracts in Natural Philosophy, Vol. 11, Springer-Verlag, New York, 1967.
10. M. M. Lavrentiev, Numerical solution of conditionally Properly posed problems, *in* "Numerical Solution of Partial Differential Equations-II," (B. Hubbard, Ed.), Academic Press, New York, 1971.
11. Y. M. Chen and J. Surmont, Iterative algorithms for constructing approximate solutions of Nonlinear problems from inadequate and erroneous data, *J. Math. Anal. Appl.*, to appear.
12. B. J. Conrath, Vertical resolution of Temperature profiles obtained from remote radiation measurements, *J. Atmos. Sci.* **29** (1972), 1262–1271.

13. Y. M. CHEN, H. M. WOOLF, AND W. L. SMITH, Vertical Resolution of Temperature Profiles for High Resolution Infrared Radiation Sounder (HIRS), to appear as a NOAA technical report.
14. L. V. KANTOROVICH AND G. P. AKILOV, "Functional Analysis in Normed Spaces," (D. E. Brown, Tr.), Pergamon Press, Oxford, 1964.

Printed in Belgium